npj | biofilms and microbiomes

Article

Published in partnership with Nanyang Technological University

https://doi.org/10.1038/s41522-025-00677-y

Age-related alterations in gut homeostasis are microbiota dependent

Yingli Jing[1,2], Qiuying Wang[1,2], Fan Bai[1,2], Zihan Li[1,2], Yan Li[1,2], Weijin Liu[1,2], Yitong Yan[1,2], Shuangyue Zhang[1,2], Chen Gao[1,2] & Yan Yu[1,2]

Accumulating data suggest that remodeling aged gut microbiota improves aging-related imbalance in intestinal homeostasis. However, evidence in favor of the beneficial effect of remodeling gut microbiota on intestinal stress and immune responses during aging is scarce. The current study revealed that old mice presented impaired gut barrier integrity. Transcriptome sequencing coupled with bioinformatics analysis revealed that aging altered gene expression profiles of the colon and mesenteric lymph nodes, which are involved mainly in stress and immune responses, respectively. Notably, gut microbiota was closely related to the differentially expressed genes. Microbiota depletion in old mice ameliorated gut barrier integrity and partially reversed the inflammatory factors upregulated in aging mice. Furthermore, fecal microbiota transplantation from young mice to old mice resulted in a significant improvement in intestinal barrier integrity and immune homeostasis. These findings highlight the potential of microbiota-targeted interventions on aging-related physiological processes and call for further investigation.

Aging is a complex, progressive process driven mostly by the accumulation of DNA damage, metabolic alterations in cells, the activation of chronic inflammation, and intestinal microbiota dysbiosis, all of which culminate in the systemic deterioration of multiple organs[1,2]. The integrity of intestinal function is crucial for the well-being of an organism throughout its lifespan. In recent years, increasing researches have focused on aging-associated intestinal dysfunction[3–6]. Intestinal aging is characterized mainly by the destruction of the intestinal barrier[7]. The intestinal barrier comprises chemical, mechanical, immune, and biological barriers, which together orchestrate ion and nutrient trafficking, immune modulation, and the intricate balance of gut microbiota diversity[8]. As the aging phenomenon progresses, the protective mucosal layer becomes thinner, and the expression of tight junction proteins, such as Occludin and ZO-1, decreases[9]. This disruption of physical barriers alters the microenvironment of bacterial growth, leading to excessive proliferation of harmful bacteria, thereby facilitating the influx of antigen-related and toxic metabolites in the circulation[10]. Clinical experiments and basic research on animal models have demonstrated that aging alters the composition of gut microbiome[11–14]. An imbalance in gut microbiota structure alters the metabolism of intestinal epithelial cells, causing sustained inflammation in the intestine[15]. These observations suggest the existence of a feedback loop in which microbial dysbiosis drives the aging process. In addition, gut microbiota critically affects the regulation of systemic immune responses and intestinal function in both health and disease.

The intestines are among the main target organs of stress in the human body, and approximately 70–80% of immune cells are located within the intestine[16]. Interventions targeting the gut microbiota, including antibiotics, probiotics, and fecal microbiota transplantation (FMT), have provided both direct and indirect evidence in favor of the importance of gut microbiota in maintaining intestinal integrity and immunity. Aimée Parker and colleagues reported that the transfer of microbiota from a young donor to aged mice ameliorated the aging-related breakdown of epithelial barrier integrity and systemic inflammation[17]. Marcus Boehme and colleagues reported that FMT of the microbiota derived from young donors could improve aging-induced immune impairments[18]. Furthermore, the administration of *Akkermansia muciniphil*a to aged mice alleviated aging-induced damage to intestinal barrier function and limited the infiltration of proinflammatory molecules[19]. A study demonstrated that beneficial commensals, such as *Christensenellaceae* and *Bifidobacteria*, could improve age-related immune and homeostasis impairments[20]. Antibiotic-mediated microbiota depletion was demonstrated to inhibit the aging-related upregulation of proinflammatory cytokines, such as IFN-γ and IL-17a, in the choroid plexu[21]. Therefore, the scientific community has developed a renewed interest in the interplay between the microbiota and immune alterations along with gut homeostasis during the lifespan of an organism.

[1]China Rehabilitation Science Institute, China Rehabilitation Research Center, Beijing Key Laboratory of Neural Injury and Rehabilitation, and School of Rehabilitation Medicine, Capital Medical University, Beijing, China. [2]Center of Neural Injury and Repair, Beijing Institute for Brain Disorders, Beijing, China.
e-mail: yuyancrrc@163.com

The intricate relationships among gut microbiota, intestinal integrity, and the intestinal immune response remain a priority topic in aging-related research. Therefore, the present study aimed to understand the impact of gut microbiota remodeling via antibiotic administration and FMT on intestinal homeostasis in aged mice while identifying the aging-related intestinal genes that might be responsible for the observed changes.

Results

Aging-related intestinal permeability was decreased

Aging-related gut dysfunction is reflected in impaired intestinal barrier integrity and an enhanced inflammatory response. When FITC-labeled dextran (4 kDa) was administered via gavage to assess intestinal barrier integrity, the plasma fluorescence intensity significantly increased in aged mice but decreased in young mice (Fig. 1a). Moreover, the levels of barrier-related tight junction proteins (ZO-1 and Occludin) were lower in aged mice than in young mice (Fig. 1b–e). These data indicated that gut permeability was significantly greater in aged mice than in control mice, potentially due to the decreased expression of tight junction components.

Aging altered the gene expression profile of the colon of the mice

The molecular mechanism underlying the effect of aging on gut function was explored next, for which colonic RNA sequencing was performed to identify the DEGs between aged and young mice. The volcano map and heatmap generated using the results obtained in the differential expression analysis of young vs. aged mice are depicted in Fig. 2a, b. A total of 85 DEGs (p-adjust ≤ 0.05; |log2FC| ≥ 1) were identified, among which 33 genes were markedly upregulated, and 52 genes were significantly downregulated in the aged mice. Next, the DEGs were subjected to traditional bioinformatics analysis using the target set, which included gene ontology (GO) functional enrichment analysis, gene set enrichment analysis (GSEA), etc. GO functional enrichment analysis revealed that the evaluated gene sets were involved in the immune response, regulation of the immune response, the innate immune response, the response to bacteria, and the defense response to bacteria (Fig. 2c). The GSEA results demonstrated that aging upregulated pathways related to inflammation, such as the adaptive immune response, lymphocyte activation, and the regulation of cell activation, including the regulation of leukocyte activation and the regulation of lymphocyte activation (Fig. 2d). Whether the cellular composition also varies between aged and young mice was investigated by performing cell-type deconvolution using CIBERSORTx[22], which revealed the proportions of various cell types in different tissues. The results obtained for the colon samples revealed no significant differences in the estimated relative proportions of the leukocyte subtypes between young and aged mice (data not presented). The gut is a target organ sensitive to stress in the human body. Therefore, the DEGs related to the response to stress between young and aged mice were investigated. The heatmap generated from the results revealed 14 DEGs whose expression was upregulated and 31 DEGs whose expression was downregulated in young mice compared with aged mice (Fig. 2e). Among these DEGs, Adig, Bex1, Cfd, Cyp2e1, Lpl, and Mrap were significantly downregulated in aged mice compared with young mice, and these DEGs were related mainly to energy metabolism, cell cycle regulation, and the complement pathway. On the other hand, Cxcr6, Gbp6, H2-M2, Ido1, Ccl21d, and Pdx1 were significantly upregulated in aged mice compared with young mice, and these DEGs were related mainly to the immune response and immune regulation (Fig. 2e). The above data suggest that with aging, the ability of the intestine to restore homeostasis decreases, which gradually leads to a chronic inflammatory state.

Aging altered the gene expression profile of mesenteric lymph nodes (MLNs)

Most immune cells (70–80%) in the human body are located in gut-related lymphoid tissues. (GALTs). MLNs play an important role in GALTs. Therefore, the gene expression profiles of MLNs were determined for both young and aged mice. The volcano map and heatmap generated using differential expression analysis between young and aged mice are presented in Fig. 3a, b. A total of 737 DEGs (p-adjust ≤ 0.05; |log2FC| ≥ 1) were

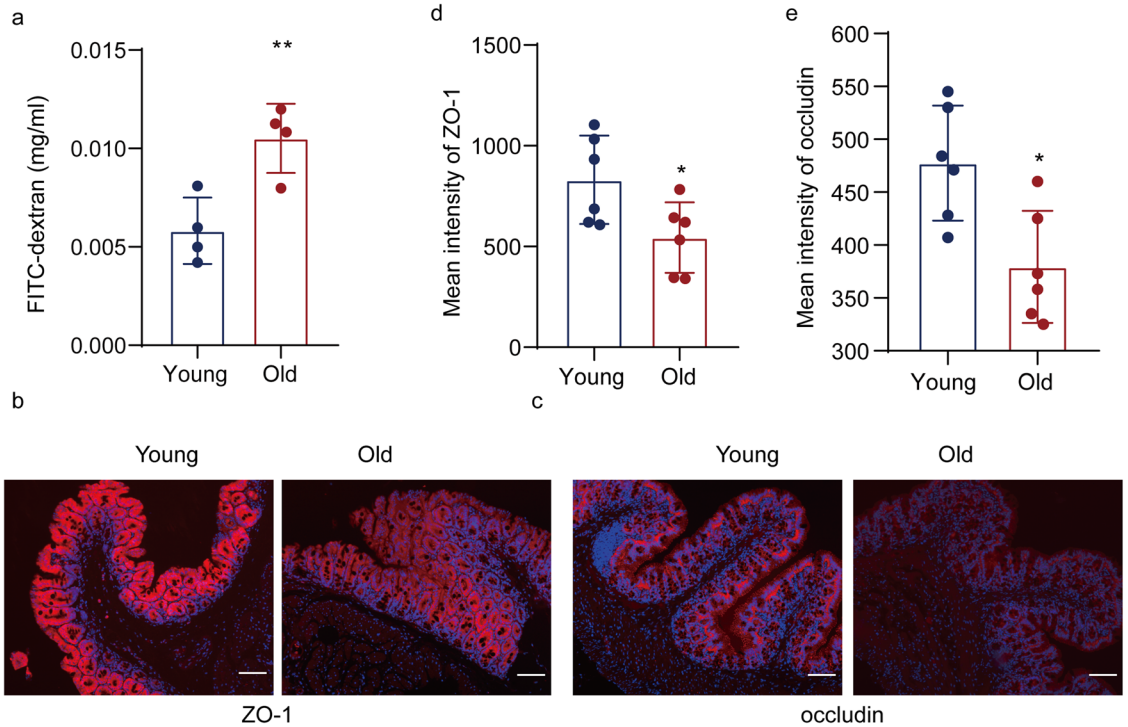

Fig. 1 | Aging is accompanied by a decline in intestinal function. a Intestinal permeability was assessed by measuring the FITC intensity in serum after oral gavage of FITC-dextran. **b**, **c** Quantification of ZO-1 and Occludin immunoreactivity (red), with representative immunofluorescence microscopy images of the colon. **d**, **e** Quantification of ZO-1 immunoreactivity and Occludin immunoreactivity (red), with representative immunofluorescence microscopy images of the colon. DAPI, blue; scale bar, 50 μm.

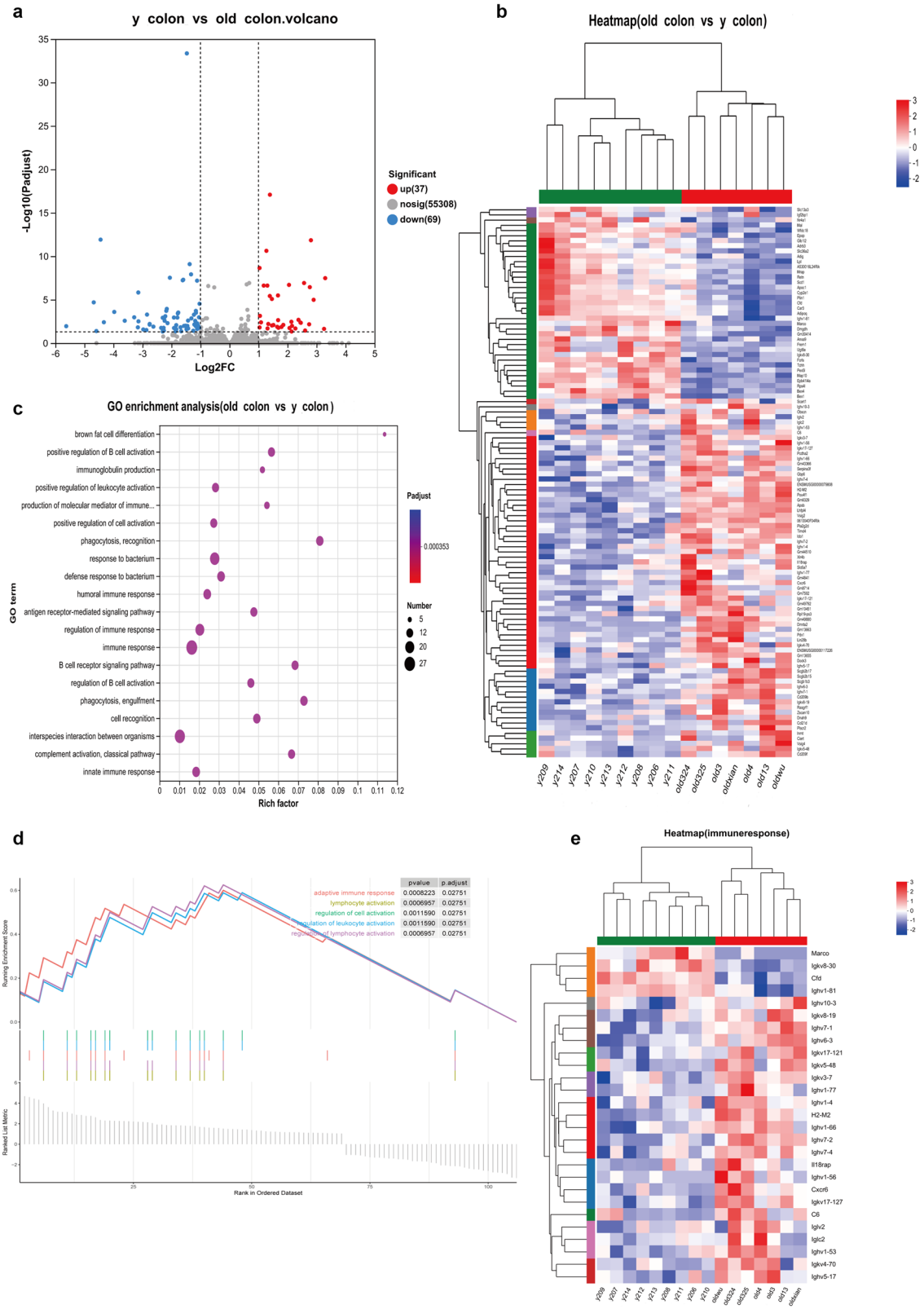

Fig. 2 | Aging-induced alterations in gene expression within the colon tissue of mice. a Volcano plot illustrating the differential (upregulated and downregulated) genes in the colon between aged and young mice. Green indicates downregulated genes; red indicates upregulated genes; gray indicates non-differentially expressed genes (no signal). **b** Heatmap illustrating the DEGs in the colon between aged and young mice. **c** GO enrichment analysis revealed the DEGs between young and aged mice; the size of each bubble is proportional to the number of DEGs assigned to the GO terms. **d** Enrichment plot of the DEGs identified in the GSEA of the colon, depicting the profile of the running enrichment score and the positions of gene set members on the rank-ordered list. **e** Heatmap depicting the expression of genes associated with the response to stress, as detected using RNA-seq.

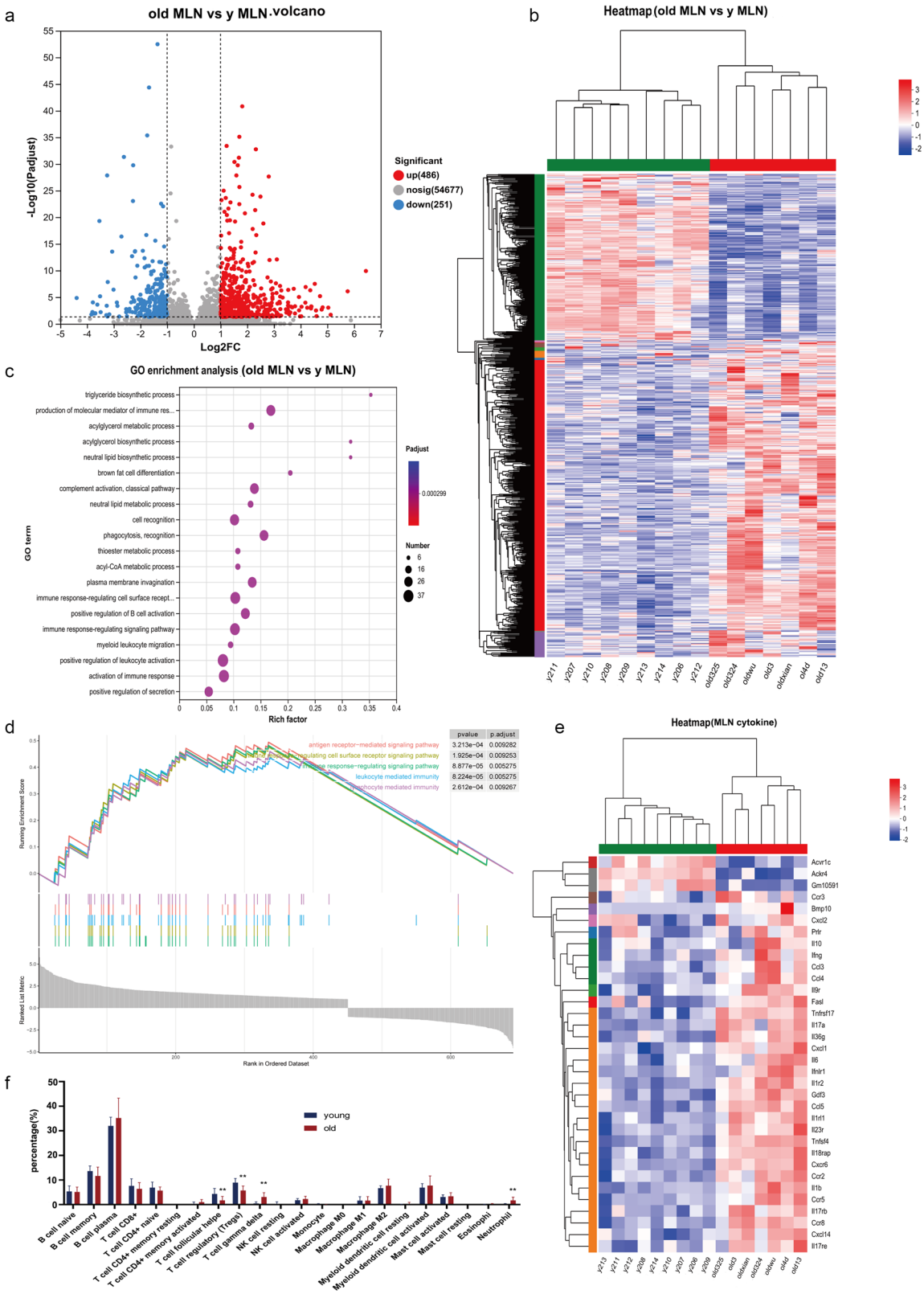

Fig. 3 | Aging-related alterations in gene expression within the MLNs of mice. **a** Volcano plot illustrating the differential (upregulated and downregulated) genes in the colon between aged and young mice. Green indicates downregulated genes; red indicates upregulated genes; gray indicates non-differentially expressed genes (no signal). **b** Heatmap illustrating the DEGs in the colon between aged and young mice. **c** GO enrichment analysis revealed the DEGs between young and aged mice; the size of each bubble is proportional to the number of DEGs assigned to the GO terms. **d** Enrichment plot of the DEG sets revealed in the GSEA of the MLNs, depicting the profile of the running enrichment score and the positions of the gene set members on the rank-ordered list. **e** Quantitative analyses of the relative abundance of the 22 digital cell types that differ between young and old mice via digital cytometry were conducted via CIBERSORTx, $^{**}p < 0.01$. **f** Heatmap depicting the expression of genes related to the cytokine-cytokine receptor interaction pathway, as detected via RNA-seq.

identified, among which 486 genes were markedly upregulated and 251 genes were significantly downregulated in aged mice. Next, the DEGs were subjected to traditional bioinformatics analysis using the target set, including GO functional enrichment analysis and GSEA. The GO enrichment analysis revealed that the DEGs were enriched mainly in pathways related to the immune response, such as the production of molecular mediators of the immune response, the immune response-regulating cell surface receptor signaling pathway, the immune response-regulating signaling pathway, positive regulation of leukocyte activation, and activation of the immune response (Fig. 3c). The GSEA results revealed enrichment of the upregulated pathways associated with aging, particularly the antigen receptor-mediated signaling pathway, the immune response-regulating cell surface receptor signaling pathway, the immune response-regulating signaling pathway, and leukocyte- and lymphocyte-mediated immunity (Fig. 3d). Protein-protein interaction network analysis of the DEGs associated with the enriched cytokines revealed that FasL, Cxcl2, Ccr8, Ccr3, Ccl4, Cxcr6, Ccl3, Ccr5, Ccr2, Cxcl1, Ccl5, IL-10, IL-1b, IL-17a, IL-6, and TNF-γ were hub genes (Supplementary Fig. 1). Next, cell-type deconvolution was performed using CIBERSORTx[22]. A comparison of the results between young and aged mice revealed that the evaluated tissue samples had 22 leukocyte subtypes with different estimated relative proportions (Fig. 3e). In particular, four cell types, namely, neutrophils, T follicular helper (T_h) cells, T-cell regulatory (Treg) cells, and T-cell gamma delta (γδ) T cells, were significantly different between young and aged mice (Fig. 3e). Heatmap visualization revealed that most of the genes encoding cytokines and chemokines were significantly upregulated in aged mice (Fig. 3f) and were associated with an increased inflammatory response to senescence. Subsequent analysis of the DEGs related to the cytokine-cytokine receptor interaction pathway revealed 3 DEGs whose expression was upregulated and 31 DEGs whose expression was downregulated in young mice compared with aged mice (Fig. 3f). Among these DEGs, Cxcl2, Ccr8, Ccr3, Ccl4, Cxcr6, Ccl3, Ccr5, Ccr2, Cxcl1, Ccl5, IL10, IL-1β, IL17a, IL6, and Ifng were significantly upregulated in aged mice compared with young mice. These findings collectively demonstrated that the proportion of immune regulatory cells significantly decreased while the proportion of proinflammatory cells significantly increased in aged mice, which was consistent with the upregulation of cytokines with the advancement of aging.

Correlation between the differentially expressed genes and the microbiota

The DEGs between the young and aged mouse groups in the colon and MLNs underscored an intriguing relationship between aging-related gene expression changes and alterations in gut microbiota. According to previous data obtained by our research group[23], the relative abundance of commensal microbiota, such as *Lactobacillus*, *Dubosiella*, and *Bifidobacteriales*, was significantly decreased in aged mice, whereas the relative abundance of commensal microbiota, such as *Alistipes*, *Bacteroides*, and *Clostridium*, was distinctly increased in aged mice. A correlation analysis was subsequently conducted in the present study to determine the associations between the DEGs in the colon/MLNs and the microbiota (Fig. 4). The heatmap generated via this correlation analysis revealed that the DEGs enriched in the colon of young mice, such as Adig, Bex1, Cfd, Cyp2e1, Lpl, and Mrap, were positively correlated with *Prevotellaceae*_UCG-001, *Dubosiella*, and *Lactobacillus* and negatively correlated with *Bacteroides*. The immune-related DEGs, such as Cxcr6, Gbp6, H2-M2, Ido1, Pdx1, and Ccl21d, which were significantly upregulated in the colon of aged mice compared with young mice, were positively correlated with the relative abundance of *Bacteroides* and negatively correlated with the relative abundances of *Prevotellaceae*_UCG-001, *Dubosiella*, and *Lactobacillus* (Fig. 4a). Similarly, cytokines and chemokines such as Fasl, Cxcl2, Ccr8, Ccr3, Ccl4, Cxcr6, Ccl3, Ccr5, Ccr2, Cxcl1, Ccl5, IL10, IL1b, IL17a, IL6, and Ifng, which were significantly upregulated in the MLNs of aged mice compared with young mice, were positively correlated with the relative abundances of *Bacteroides* and *Alistipes* and negatively correlated with the relative abundances of *Prevotellaceae*_UCG-001, *Dubosiella*, and *Lactobacillus* (Fig. 4b).

Microbiota depletion restored aging-dependent gut functional defects

Considering the pivotal role of the microbiota in regulating gut barrier integrity and influencing gut-mediated inflammation, the impact of intestinal microbiota depletion on intestinal permeability was investigated next in the present study. As depicted in Fig. 5a, the permeability of the gut barrier was significantly greater in aged mice than in young mice, and this effect was reversed after exposure to the antibiotic. Moreover, the permeability of the gut barrier in young mice did not differ significantly with or without exposure to antibiotics. Next, the expression of tight junction proteins in the colon was estimated. Consistent with the leaky gut phenotype, the colons of aged mice presented reduced gene expression of ZO-1 and Occludin. However, antibiotic exposure significantly upregulated the expression of ZO-1, whereas the expression of Occludin remained unaffected (Fig. 5b, c). Conversely, the gene expression levels of ZO-1 and Occludin in young mice did not differ significantly with or without exposure to the antibiotic. The extent to which intestinal microbiota depletion impacted the intestinal immune response-related DEGs between young and aged mice was subsequently assessed. The PCR data revealed that the gene expression levels of H2-M2 and GBP6 were significantly greater in the aged mice than in the young mice, and a downward trend was observed following antibiotic exposure, which did not reach a statistically significant level in the aged mice (Fig. 5d, e). The gene expression of Cxcr6 demonstrated a trend similar to that of H2-M2 and GBP6 among all four groups, although no marked distinction was noted between young and aged mice (Fig. 5f). We also measured the levels of common inflammatory factors (IL-1β, TNF-α, and IL-6). The data revealed that the gene expression levels of TNF-α and IL-6 were significantly greater in aged mice than in young mice, which was reversed by microbiota depletion in old mice. With respect to the gene expression of IL-1β, there were no significant differences among the four groups (Supplementary Fig. 2). The above data suggest that the age-dependent microbiome affects the expression of certain colonic genes and thereby affecting intestinal permeability.

Microbiota depletion altered the expression of inflammation-related genes in the MLNs

Next, whether intestinal microbiota depletion was involved in the MLNs-related immune response was investigated. qRT-PCR analysis revealed that the expression of cytokine-related genes, such as Ccr2, Ccr3, Ccr5, Cxcr6, and IFN-γ, was increased in the MLNs of aged mice. However, antibiotic exposure significantly downregulated the expression of Ccr2, Ccr3, Cxcr6, and IFN-γ but not the expression of Ccr5 toward the levels recorded in young mice. Furthermore, the gene expression levels of Ccr2, Ccr3, Ccr5, Cxcr6, and IFN-γ in young mice were not evidently altered regardless of exposure to the antibiotic (Fig. 6a–d, h). In addition, the expression of Ccr8, Ccl3, Ccl4, and Il-17A did not significantly differ among the four groups (Fig. 6e–g, i). These findings suggested that microbiota depletion partially altered the expression of immune response-related genes in the MLNs and alleviated the inflammatory microenvironment in the intestine.

FMT from young mice reversed the aging-dependent breakdown of epithelial barrier integrity and intestinal inflammation

The data above demonstrated that the alteration of gut microbiota affected gut homeostasis. Furthermore, we designed rescue experiments involving the transplantation of microbiota from young mice into old mice (YO group) and the transplantation of microbiota from old mice into old mice (OO group) to observe the effect of the young gut microbiota on the intestinal function of old mice. Figure 7a shows that the intestinal barrier integrity of old mice improved with the intervention of young gut microbiota. Additionally, young gut microbiota transplantation markedly restored the expression of ZO-1 and Occludin (Fig. 7b). The PCR data revealed that the transplantation of microbiota from

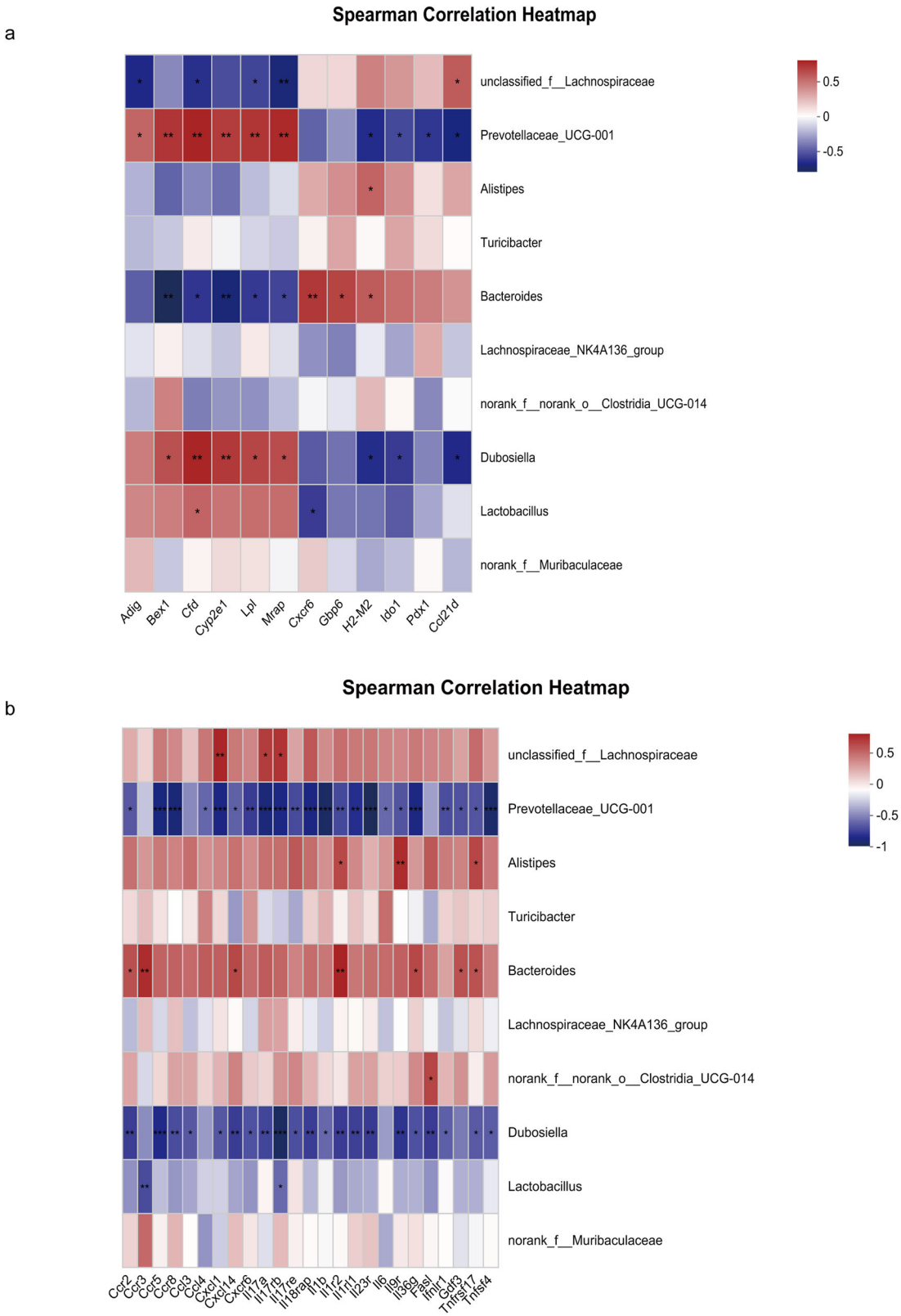

Fig. 4 | Correlations between the DEGs and community composition. a Heatmap analysis of the correlation results obtained for the DEGs identified in the colon and the community composition between young and aged mice at the genus level. **b** Heatmap analysis of the correlation results obtained for the DEGs identified within MLNs and the community composition between young and aged mice at the genus level. $^{*}p < 0.05$; $^{**}p < 0.01$.

young mice into old mice significantly reversed the old-induced increase in TNF-α and IL-6 levels but not in the expression of H2-M2, Gbp6, Cxcr6, and IL-1β in the colonic tissue (Fig. 7b). Moreover, the PCR data revealed that age-induced increases in Ccr3, Ccl3, Ccl4 and IFN-γ, which were mediated by the transplantation of microbiota from young mice into old mice in MLNs (Fig. 7c). These data demonstrated that the young gut microbiota exerted a protective effect on intestinal barrier integrity and gut homeostasis.

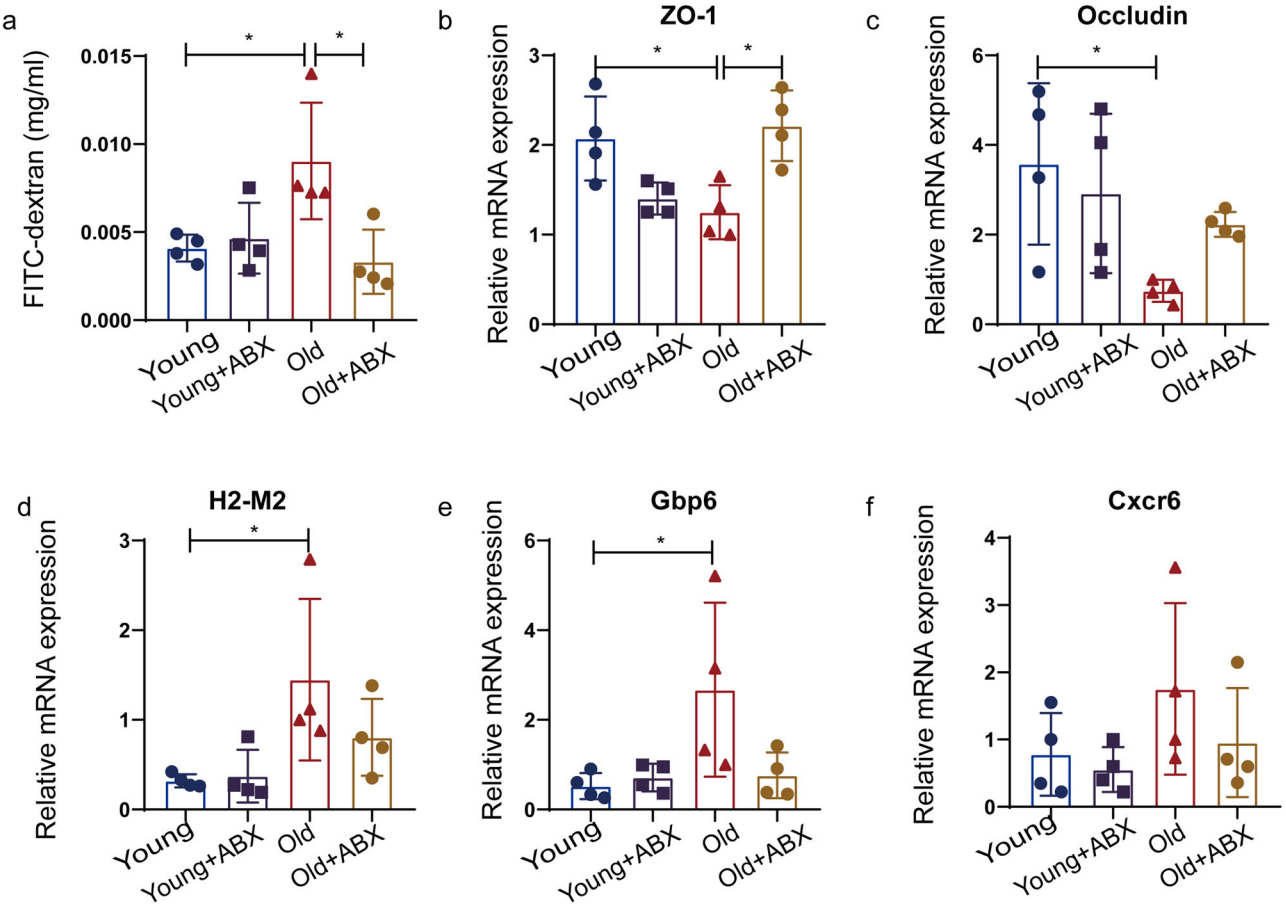

Fig. 5 | Microbiota depletion altered gut permeability and the expression of colon-related genes. a Intestinal permeability was assessed by measuring the FITC intensity in the serum after oral gavage of FITC-dextran in young and aged mice with and without antibiotic exposure. **b**, **c** The expression levels of tight junction genes (ZO-1 and Occludin) in the colon were determined through quantitative PCR. **d**–**f** The expression levels of intestinal stress response genes (H2-M2, Gbp6, and Cxcr6) in the colon were determined through quantitative PCR; $*p < 0.05$ compared with the aged mice group; $**p < 0.01$ compared with the aged mice group (ABX: antibiotic cocktail treatment).

Discussion

Gut homeostasis and gut microbiome have attracted increasing attention in the context of research on the pathophysiological mechanism underlying aging. In the present study, the features of aging-related changes in the gene expression profiles of the colon/MLNs were revealed through RNA sequencing. Furthermore, the regulatory effects of gut microbiome on gut homeostasis were explored by using microbiome depletion and FMT from young to aged mice. The results revealed that gut microbiota influences the expression characteristics of certain genes in the colon and MLNs with increasing age while also regulating gut barrier integrity in aged mice. These findings suggest that targeting gut microbiota could be used as a novel intervention strategy with the potential to reverse immune aging and thereby enhance the overall health of older individuals.

Both clinical studies on aging and research using animal models of aging have reported that intestinal function is disrupted with advancing age. Reduced intestinal barrier integrity, decreased expression of tight junction proteins, and altered intestinal tissue morphology contribute to intestinal dysfunction[24]. In the present study, aged mice presented increased intestinal barrier permeability and decreased expression of the tight junction protein ZO-1. The intestinal barrier is composed of an overlying mucus layer, epithelial cells, and lamina propria. Epithelial cells are interconnected through tight junction proteins [zonulin and occludin] to prevent pathogens and toxins from infiltrating the epithelium[25]. A study in non-human primate models reported that age-associated remodeling of intestinal epithelial tight junctions (such as ZO-1 and Occludin) was a pivotal contributing factor to the increased permeability of the intestinal barrier[26]. Jongoh Shin and colleagues reported that an increase in systemic inflammation and a decrease in the expression of genes encoding barrier-forming tight junction proteins (ZO-1, Cldn3, and Cldn4) were accompanied by an age-dependent increase in intestinal permeability[19]. The administration of *Akkermansia muciniphila* improves intestinal integrity and homeostasis by decreasing systemic inflammation and increasing the expression levels of tight junction proteins[19]. Furthermore, reshaping gut microbiota of elderly mice ameliorated intestinal barrier integrity and reduced inflammation[17,27]. These findings suggest that intestinal inflammation may be an important trigger and intervention target for age-associated disruption of intestinal barrier function. Furthermore, transcriptomic analysis revealed differences in the colons of young and aged mice. GO enrichment analysis revealed that most of the DEGs were enriched in immune response-related signaling pathways. Proinflammatory factors, such as H2-M2, Gbp6, and Cxcr6, are highly expressed in the colons of aged mice. H2-M2 is a conserved mouse class Ib gene that is translated into a surface-expressed MHC class I molecule, suggesting a role in the immune system[28]. Gbp6 is an interferon-inducible guanylate-binding protein (GBP) family gene. The upregulation of GBP6 was observed in experimental models of multiple sclerosis and myocarditis patients and was shown to have an important effect on the inflammatory axis, contributing to the pathogenesis of diseases[29,30]. GBP6 is also involved in inflammation- and apoptotic-related processes and might be a potential therapeutic target for nanoparticle-induced retinal injury[31]. CXC chemokine receptor 6 (CXCR6), a seven-transmembrane domain G protein-coupled receptor, plays a pivotal regulatory role in inflammation and tissue damage[32]. CXCR6 is highly expressed in the colon of patients with Crohn's

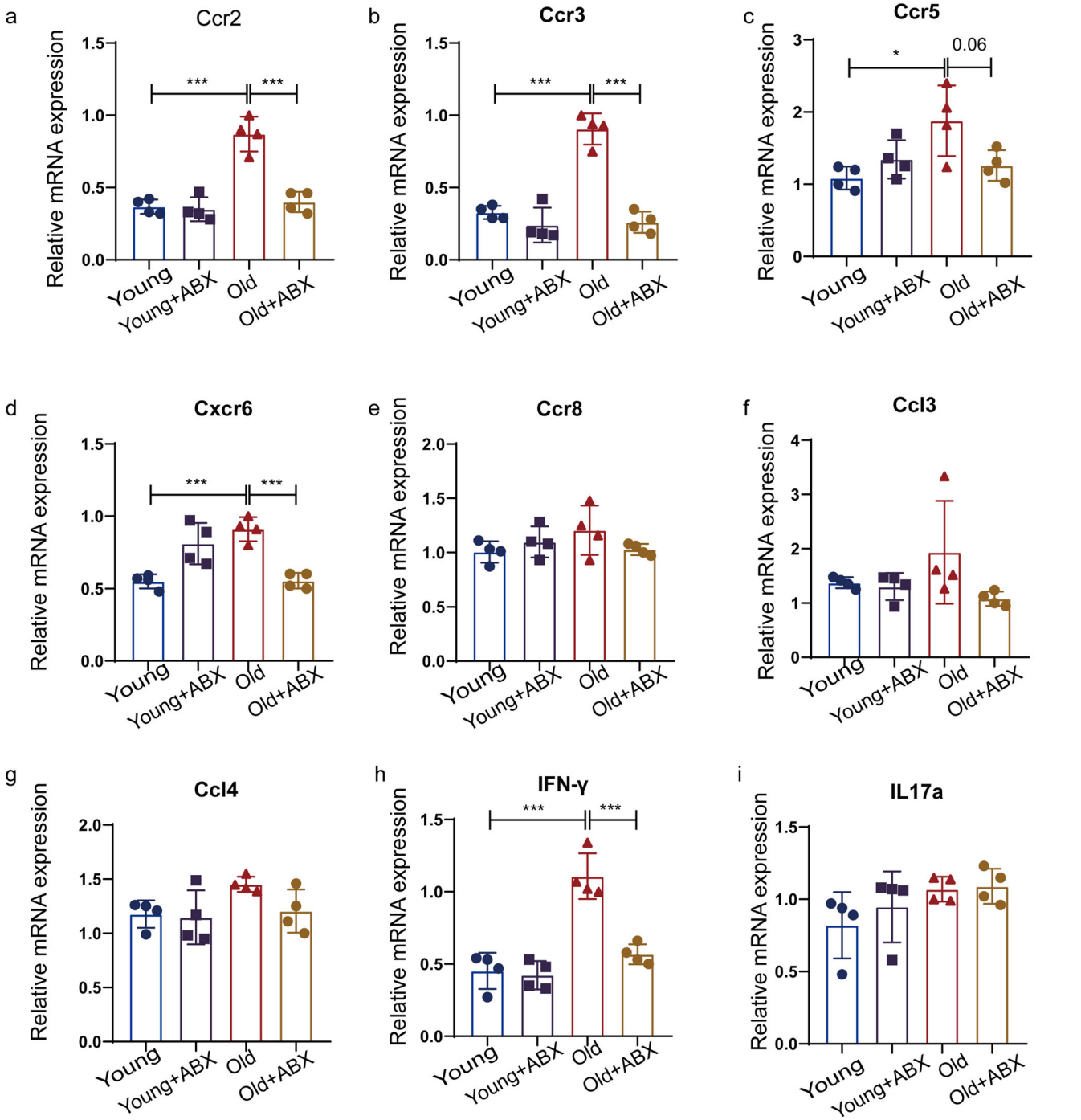

Fig. 6 | Microbiota depletion altered the expression of genes associated with the MLN-related immune response. a–i The expression levels of intestinal immune response genes (Ccr2, CcR3, Ccr5, Cxcr6, Ccr8, Ccl3, Ccl4, IFN-γ, and IL-17a) in the MLN were determined through quantitative PCR; $^{*}p < 0.05$ compared with the aged mice group; $^{**}p < 0.01$ compared with the aged mice group.

disease (CD)[33] and in the inflamed small intestine of mice[34]. Although evidence shows that these genes are involved in immune regulation, inflammation, and tissue damage, the correlation between the three genes and the intestinal barrier still needs to be elucidated.

Gut dysbiosis might also activate mucosal immune cells in the GALT, thereby affecting systemic inflammation[35]. The MLNs are the most prominent region for immune activation in GALT and, therefore, serve as a firewall between the intestine and other regions in the body[36]. MLNs are sentinel sites of enteral immunosurveillance and immune homeostasis[37]. Therefore, transcriptomic analysis of MLNs was subsequently performed. GO enrichment analysis revealed that the DEGs were enriched in immune response functions. The MLNs contain many types of immune cells, with multiple immune-related receptors on the surface, and can secrete different cytokines and chemokines under different conditions[38]. We found that among the numerous differentially expressed cytokines in young and elderly MLNs, cytokines such as FasL, Cxcl2, Ccr8, Ccr3, Ccl4, Cxcr6, Ccl3, Ccr5, Ccr2, Cxcl1, Ccl5, IL-10, IL-1β, IL-17a, IL-6, and TNF-γ play important roles through PPI analysis. Ccr2-dependent monocytes exacerbate intestinal inflammation, and targeting $Ccr2^{+}$ monocyte-dependent responses could provide a better understanding of TBI-induced gut inflammation[39]. In

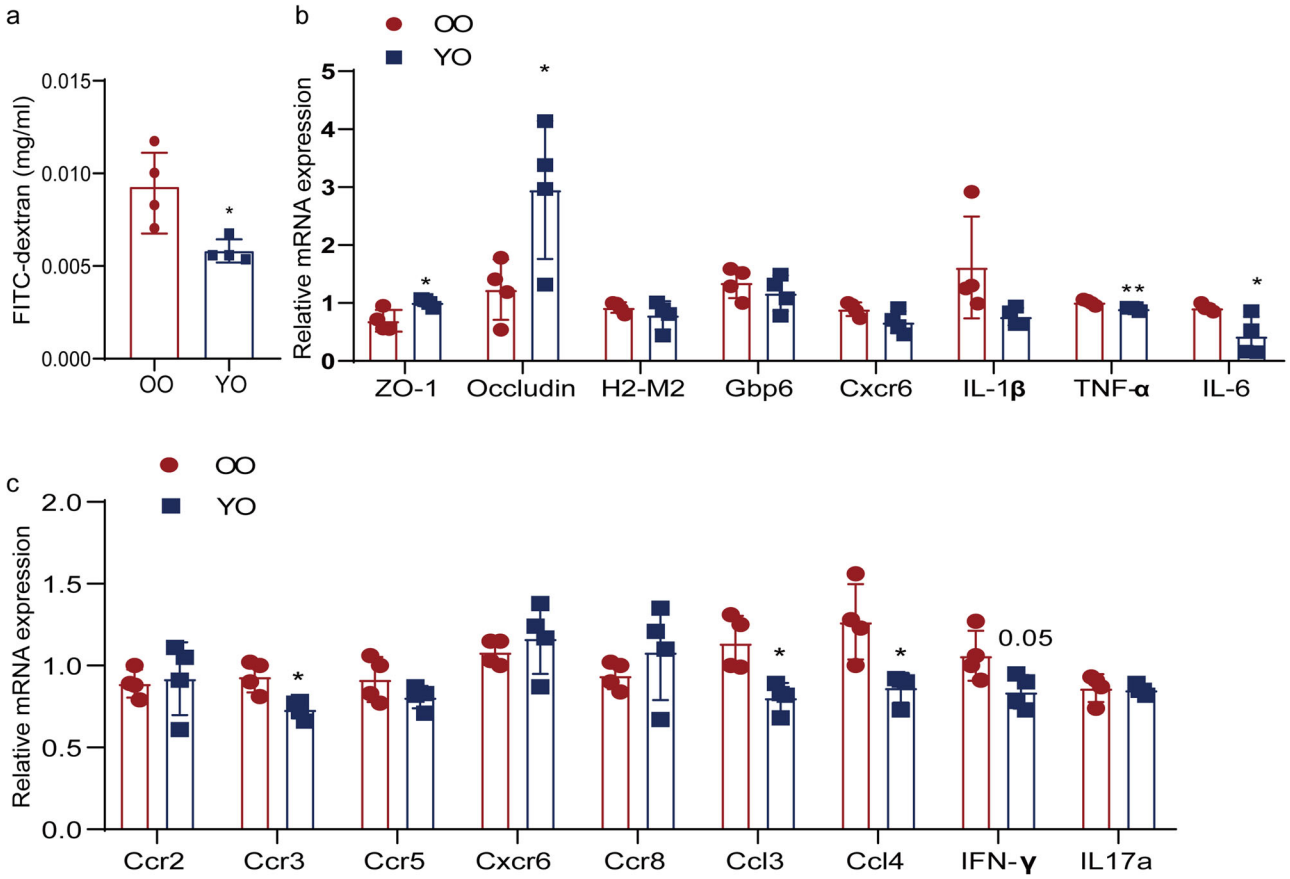

Fig. 7 | Young gut microbiota protected the intestinal barrier and reduced inflammation. a Intestinal permeability was assessed by measuring the FITC intensity in the serum after oral gavage of FITC-dextran in the OO and YO groups. **b** The expression levels of tight junction genes (ZO-1 and Occludin) and H2-M2, GBP6, CXCR6, IL-1β, TNF-α and IL-6 in the colon were determined through quantitative PCR. **c** The expression levels of Ccr2, Ccr3, Ccr5, Cxcr6, Ccr8, Ccl3, Ccl4, IFN-γ, and IL-17a in the MLN were determined through quantitative PCR; $^{*}p < 0.05$ compared with the OO group; $^{**}p < 0.01$ compared with the OO group (OO: transplantation microbiota from old mice into old mice; YO: transplantation microbiota from young mice into old mice).

the inflamed colons of CD patients, $Ccr2^{+}$ and $Ccr5^{+}$ $CD4^{+}$ T cells are enriched, whereas Cenicriviroc, a dual Ccr2/Ccr5 antagonist, displays a protective effect in experimental colitis models by inhibiting the generation of the proinflammatory cytokines IFN-γ, IL-17, IL-6, and IL-1β during colitis, which further prevents intestinal inflammation and preserves epithelial barrier integrity[40]. In Ccr2-deficient mice, the infiltration of Th2-type T cells in the lamina propria is absent, but increased levels of IL-10 and decreased levels of IFN-γ may downregulate mucosal inflammation[41]. The chemokine receptor Ccr3 plays a pivotal role in the local and systemic recruitment and activation of eosinophils. However, targeting eosinophils via the Ccr3 axis has anti-inflammatory effects on the inflamed intestine[42]. Inhibition of the Ccr3-eotaxin axis prevents inflammation-induced functional changes in the gastrointestinal tract[43]. Intestinal lymphocytes are responsible for immune effector functions and can be modulated by certain probiotics. *Bifidobacterium pseudocatenulatum* CECT7765 decreases the expression of the proinflammatory chemokine receptors Ccr6, Ccr9, Cxcr3 and Cxcr6 and reduces intestinal permeability, which contributes to improved gut homeostasis in experimental chronic disease[44]. IFN-γ induces the recruitment of Th1 cells to the proinflammatory chemokine Cxcl10/IP10 in the primary murine intestinal crypt epithelium[45]. Furthermore, IFN-γ induces a decrease in the permeability of the intestinal barrier and morphological disruption of tight junctions in intestinal epithelial cells[46]. The literature has demonstrated that multiple cytokines can mediate intestinal inflammation, which further affects intestinal integrity. The application of CIBERSORTx revealed that the proportion of immune regulatory cells (T_h cells and Tregs) was significantly decreased in aged mice, whereas the proportion of proinflammatory cells (neutrophils and γδ T cells) was significantly increased in these mice. These observations were consistent with the upregulation of cytokines in the MLNs with advancing age. The above findings underscore the intricate interplay among aging, gut microbiota, and immune dysregulation, providing insights into the potential mechanisms underlying aging-related intestinal dysfunction and systemic inflammation.

The colon serves as a barrier tissue and presents a unique immune environment in which immune cells exhibit tolerance toward various microbial communities, which are collectively referred to as the microbiome. The microbiome is important for several aspects of health, and an imbalance between the commensals and the pathogenic microbiota is associated with several disease states[47,48]. The intestinal microbial composition and abundance are dramatically altered with advancing age, which could promote the onset of chronic diseases[49]. In the present study, proinflammatory factors were highly expressed in the colon and MLNs of aged mice, and these factors were negatively correlated with beneficial symbiotic bacteria, such as *Prevotellaceae*_UCG-001 and *Dubosiella*, and positively correlated with *Alistipes* and *Bacteroides*. L-Arabinose attenuates LPS-induced intestinal inflammation and injury by partly restoring the abundance of *norank_f__Muribaculaceae, Faecalibaculum, Dubosiella, Prevotellaceae_UCG-001*, and *Paraasutterella*[50]. Deferasirox alleviates DSS-induced ulcerative colitis in mice by increasing the abundance of *Prevotellaceae_UCG-001, norank_f__Muribaculaceae, Lachnospiraceae_NK4A136_group, Odoribacter* and *Blautia*[51]. Yanan Zhang and colleagues reported that *Dubosiella* could ameliorate the immune microenvironment by downregulating the proinflammatory factors Il17 and Ifng and upregulating the anti-inflammatory factors Il10 and Tgfb, which is beneficial for the restoration

of intestinal mucosal barrier function[52]. *Alistipes* is a relatively new genus of bacteria isolated primarily from medical clinical samples. Recent studies illustrate emerging chronic intestinal immunological and mechanistic implications by which *Alistipes* correlate with dysbiosis and disease[53]. The *Bacteroides* species, on the other hand, are significant clinical pathogens detected in most anaerobic infections, with an associated mortality rate of over 19%[54,55]. The *Alistipes* and *Bacteroides* microbial communities are closely associated with intestinal inflammation and ferroptosis in iron overload-induced colitis[56]. Transplantation of HFD-fed gut microbes into normal diet-fed mice (HFD-FMT) showed a profound increase in the genera *Bacteroides* and *Prevotella*, both of which likely contributed to metabolic endotoxemia in HFD-FMT mice[57]. There was also a positive correlation between blood endotoxin and *Bacteroides* abundance[57]. Yi Wan and colleagues reported that a diet with a relatively high fat content was associated with an increased abundance of *Alistipes* and *Bacteriodes* and induced relatively high levels of proinflammatory factors in the plasma, suggesting the potential role of these bacteria in the metabolic health of the host[58]. Studies have suggested that the commensal microbiota might maintain gut homeostasis by modulating intestinal inflammation, which plays a critical role in affecting human health.

Increasing evidence suggests that the transfer of fecal microbiota from young mouse donors or gut microbiota depletion achieved using an antibiotic cocktail could reshape gut function toward the alleviation of aging-related deficits[17,21]. Intriguingly, the results of the present study demonstrated that antibiotic treatment of aged mice reversed the impairment of gut barrier integrity induced by aging. The intestinal stress response and immune microenvironment are inherently correlated with gut microbiota. In addition, qRT-PCR was performed to assess alterations in the associated DEGs in the colon and MLNs of aged mice subjected to microbiota depletion. Aging significantly increased the levels of H2-M2 and Gbp6, in addition to a tendency toward increased Cxcr6, and this difference, although not statistically significant, appeared to be reduced after microbiota exposure. These findings suggest that the gut commensal microbiome is essential for intestinal inflammation in the host. In addition, the expression of Ccr2, Ccr3, Cxcr6, and IFN-γ was increased in the MLNs of aged mice, and this difference was reduced after microbiota depletion. Furthermore, aging significantly increased the expression of Ccr5, in addition to a tendency toward increased Ccl3 and Ccl4 expression, and this difference, although not significantly different, appeared to be reduced after microbiota exposure. Liu et al. reported that stroke could induce macrophages derived from the intestine to express TREM1 and migrate to ischemic lesions, thereby exacerbating brain injury through secondary immune responses[59]. In addition, studies on animal models of intracranial hemorrhage and focal cerebral ischemia revealed that numerous $CD4^+$ T lymphocytes in the intestine migrated to the periphery of the intracranial hematoma and the ischemic brain region, synergistically inducing neuroimmune occurrence[60,61]. Furthermore, Joana S. Cruz-Pereira and colleagues reported that microbiota depletion could partially reduce the accumulation of $CD4^+$ T cells at the lateral and 3rd ventricles in aged mice[21]. These data suggest that abolishing intestinal microbial signals could impact the accumulation and migration of immune cells by affecting the chemotaxis of immune cells and the secretion of cytokines from these cells, although this possibility needs to be further investigated prior to reaching a conclusion.

Furthermore, a key issue regarding inflammaging and age-dependent intestinal immunity is whether age-associated changes in gut microbiota are causal in the breakdown of barrier integrity and the immune microenvironment. Our data showed that gut microbiota depletion and transplantation of young donor microbiota into old recipients led to reduced intestinal barrier permeability and restrained intestinal inflammation, supporting the positive influence of young microbiota on age-related gut immunity. In addition, gut microbiota from aged donors deteriorates inflammation and paracellular permeability[15,62]. These findings did not rule out the possibility that the progression of intestinal inflammation during aging may drive changes in gut microbiota. It has been reported that intestinal inflammation disrupts the microenvironment of gut microbiota and promotes an imbalance in gut microbiota[10,63]. Gut dysbiosis could further exacerbate the disruption of intestinal homeostasis through feedback loop mechanisms involving metabolites, neurotransmitters, cytokines, etc.[64–66].

In the context of the inextricable connection between the aged gut microbiota and changes in intestinal homeostasis, gut microbiota significantly affects intestinal metabolism and the immune response rather than affecting intestinal barrier integrity. Here, we demonstrated that removing the age-related microbiota or transplanting the microbiota from young mice into aged mice can ameliorate gut homeostasis. We further explored how gut microbiota orchestrated these improvements. Several types of gut and MLNs-associated immunity are restored following gut microbiota remodeling, suggesting that alterations in the gut microbiota in aged mice drive impairments in immune functions, which may underlie the loss of age-associated integrity in the intestinal epithelial barrier. Future studies should focus on how specific gut microbiota drive these alterations to uncover the direct mechanistic basis of the aged gut. Our data provide fundamental evidence that targeting gut microbiota may be a potential approach for treating age-associated inflammatory and functional decline.

Methods

Animals

Adult female C57BL/6J mice (3 months old) and aged female C57BL/6J mice (22 months old) were procured from the Center of Experimental Animals, Capital Medical University, Beijing, China. All the mice were housed in an air-conditioned room at a temperature of 22 ± 2 °C, a relative humidity of 55 ± 10%, and a standard 12 h light/12 h dark photoperiod. Food and water were available ad libitum to all the animals. The animal experiment protocols used in the present study were approved by the Animal Care and Use Committee of Capital Medical University (approval no. AEEI-2022-157).

Experimental grouping

Part I included 16 animals, 9 young mice, and 7 old mice. Blood was collected to test intestinal barrier permeability, colonic tissue was collected to detect Occludin and ZO-1 by immunofluorescence, and colonic and MLNs were collected for transcriptome sequencing.

Part II: Antibiotic intervention: 16 animals were divided into four groups: 8 young mice were divided into antibiotic and no antibiotic groups, with 4 animals in each group; 8 old mice were divided into antibiotic and no antibiotic groups, with 4 animals in each group; 10 days after the intervention, blood was collected to test intestinal barrier permeability, and colonic and MLNs were taken for RT-PCR to detect changes in specific inflammatory factors.

Part III: FMT intervention: 8 animals, 4 young mice and 4 old mice. Fecal microbiota from healthy young mice and old mice were respectively transplanted into old mice, which were then divided into YO and OO groups. Before FMT, mice were orally gavaged with 100 μL antibiotic cocktails for one week, containing neomycin (0.5 g/L), vancomycin (0.5 g/L), metronidazole (1 g/L), and ampicillin (1 g/L). Subsequently, mice were orally gavaged with 100 μL microbiota suspension, daily for 4 weeks. Four weeks after the intervention, blood was collected to test intestinal barrier permeability, and colonic and MLNs were collected for RT-PCR to detect changes in inflammatory factors.

FITC-dextran permeability assay

All the mice were subjected to 14 h of fasting and then administered isothiocyanate-dextran fluorescein (FITC-dextran, 4 kDa; 46944; Sigma Aldrich, Madrid, Spain; 60 g of FITC-dextran per 100 g of body weight in a volume of 0.2 mL) via gavage. After 4 h, blood samples were obtained through cardiac puncture. The collected blood in each sample was allowed to coagulate for 30 min and then centrifuged at 6000×*g* for 90 s. The resulting supernatant was diluted with an equal volume of sterile PBS, and 100 μL of the dilution was placed in a single well in a 96-well plate. The fluorescence in each well was measured using a plate reader (EnSpire; Perkin Elmer) at an excitation wavelength of 481 nm and an emission wavelength

of 524 nm. The FITC-dextran concentration was calculated using a standard curve generated through measurements conducted on the same plate.

Immunofluorescence

The mice were anesthetized using pentobarbital sodium (35 mg/kg, i.p.) and then perfused with 0.1 M PBS (pH 7.4, 37 °C) followed by 4% (w/v) paraformaldehyde in 0.1 M PBS. The colonic sections were equilibrated in 0.1 M Tris-buffered saline for 10 min, followed by incubation in 0.3% hydrogen peroxide for 30 min. Afterward, the sections were permeabilized with 0.1% Triton X-100 for 30 min. After being blocked with 10% normal goat serum in PBS for 1 h, the sections of the spinal cord were incubated with primary antibodies, namely, rabbit polyclonal anti-ZO-1 (1:100, ab216880, Abcam) or rabbit monoclonal anti-occludin (1:100, ab216327, Abcam), for 1 h. Afterward, the slides were rinsed with PBS and then incubated with the secondary antibody. The slides were then covered by placing a cover slip over a drop of glycerin-containing medium and then examined under a fluorescence microscope. The relative gray value was calculated using Image-Pro Plus 7.0 (Media Cybernetics, Silver Spring, MD, USA).

RNA extraction and sequencing

Colonic tissue (1 cm in length up to the cecocolic junction) was collected. MLNs were excised by microdissection along the length of the superior mesenteric artery lying behind the MLNs to the aortic root. Total RNA was extracted from tissues using TRIzol Reagent according to the manufacturer's instructions (Invitrogen) and then subjected to a quality assessment using a 5300 Bioanalyzer (Agilent). The extracted RNA was quantified using an ND-2000 (NanoDrop Technologies). High-quality RNA samples (OD260/280 = 1.8–2.2, OD260/230 ≥ 2.0, RIN ≥ 6.5, 28S:18S ≥ 1.0, >1 μg) were then used for library construction. RNA purification, reverse transcription, library preparation, and sequencing were performed at Shanghai Majorbio Bio-Pharm Technology Co. Ltd. following Illumina protocols. The RNAseq transcriptome library was prepared following the TruSeqTM RNA sample preparation Kit from Illumina (San Diego, CA) using 1 μg of total RNA, and the process involved mRNA isolation using poly-A selection, cDNA synthesis using random hexamer primers, and end-repair using 'A' base addition. Size-selected libraries (300 bp) were then PCR amplified and sequenced on a NovaSeq 6000 sequencer (2 × 150 bp) according to the standard protocols of Majorbio Bio-Pharm Technology Co. Ltd.

Bioinformatics analysis

Raw paired-end reads were subjected to quality trimming and control using fastp[67] with default parameters. The clean reads were then aligned to the reference genome (GRCm39) using HISAT2[68] in orientation mode. The mapped reads were assembled using StringTie[69] in a reference-based manner. A differential expression analysis was then performed using DESeq2[70], considering the differentially expressed genes (DEGs) with $|\log2FC| \geq 1$ and p-adjust ≤ 0.05, where the p-values were adjusted for multiple testing using the Benjamini-Hochberg method. Next, a functional enrichment analysis was conducted, which included the GO analysis conducted using GO TOOLS[71], with the significance established at the Bonferroni-corrected p-value of ≤0.05. The above data analysis was conducted using the free online Majorbio Cloud Platform (http://www.majorbio.com). Finally, GSEA was performed using the ClusterProfiler (4.7.1) package in R software (4.2.3), with multiple comparisons corrected using the Benjamini-Hochberg method, and the results were visualized using Enrichpolt (1.18.3).

Antibiotic treatment

Gut microbiota depletion was performed by administering an antibiotic cocktail mixed in the drinking water containing 1 g/L ampicillin, 0.5 g/L neomycin, and 0.35 g/L vancomycin to adult mice for 10 consecutive days as described in a previous study[21,72]. The antibiotics were dissolved in water, and the water was refreshed every other day. The control animals received water without antibiotics, and this water was also refreshed every other day.

Preparation of donor fecal transplant material

The fecal material was collected and isolated as previously reported[73]. Young healthy C57BL/6J mice were kept in the same housing and environmental conditions. Antibiotic-untreated young healthy mice were used as donors to collect gut microbiota. The donor fecal pellets were collected under SPF conditions. Stools from donor mice were pooled, and 100 mg was resuspended in 1 mL of sterile saline. The solution was vigorously mixed for 10 s via a benchtop vortex before centrifugation at 800×g for 3 min. The supernatant was collected and used as transplant material, as described below. Donor stool was freshly prepared on the day of transplant within 2 h before gavage administration to prevent changes in bacterial composition.

PCR array

The total RNA from the colon and MLNs was extracted using the RNA Easy Fast Tissue/Cell Kit (DP451; TIANGEN, Beijing, China) and then reverse-transcribed into cDNA using the PrimeScript RT Master Mix (RR036B; Takara, Dalian, China). Real-time qPCR was then performed on an Applied Biosystems 7500 Real-time PCR system using SYBR Premix Ex Taq (Tli RNase H Plus) (RR820A; Takara, Dalian, China) and the following primer sequences:

ZO-1: forward (5′-AGGACACCAAAGCATGTGAG-3′) and reverse (5′-GGCATTCCTGCTGGTTACA-3′);

Occludin: forward (5′-TTGGCTACGGAGGTGGCTATGG-3′) and reverse (5′-ACTAAGGAAGCGATGAAGCAGAAGG-3′);

H2-M2: forward (5′-GCCCTGGGTTTCTACCCTTC-3′) and reverse (5′-AACCAGGCCAACAGCAACTA-3′);

Gbp6: forward (5′-AGCAACTGAGAAGGAAGCTGGA-3′) and reverse (5′-GGAAAGCCTTTTGATCCTTCATTAG-3′);

Cxcr6: forward (5′-GTTTCTGCTGAACTTGCCCC-3′) and reverse (5′-CCCAAATGAGCAAGCAAATGAC-3′);

Ccr2: forward (5′-ACGATGATGGTGAGCCTTGTC-3′) and reverse (5′-TGCAGCATAGTGAGCCCAGA-3′);

Ccr3: forward (5′-CGCTATCCAGAGGGTGAAGAAG-3′) and reverse (5′-AAGGAGAACCAGGTTGTACGGG-3′);

Ccr5: forward (5′-CTGTCATCTATGCCTTTGTTGGA-3′) and reverse (5′-AGCTTGCACGATCAGGATTGTCT-3′);

Ccr8: forward (5′-GGGAACAGCCTGGTCATCTTA-3′) and reverse (5′-CACATCGCAGTCCCAAACAC-3′);

Ccl3: forward (5′-CCATATGGAGCTGACACCCC-3′) and reverse (5′-GAGCAAAGGCTGCTGGTTTC-3′);

Ccl4: forward (5′-CCCAGCTCTGTGCAAACCTA-3′) and reverse (5′-CCATTGGTGCTGAGAACCCT-3′);

IFN-γ: forward (5′-ATGAACGCTACACACTGCATCTT-3′) and reverse (5′-TGACTGTGCCGTGGCAGTAA-3′);

IL17A: forward (5′-TCCACCGCAATGAAGACCCT-3′) and reverse (5′-CATGTGGTGGTCCAGCTTTCC-3′);

IL-1β: forward (5′-AGGCTCCGAGATGAACAACAAA-3′) and reverse (5′-GTGCCGTCTTTCATTACACAGGA-3′);

TNF-α: forward (5′-CCGTCAGCCGATTTGCTATCT-3′) and reverse (5′-GCAATGACTCCAAAGTAGACCTG-3′);

IL-6: forward (5′-CCCCAATTTCCAATGCTCTCC-3′) and reverse (5′-CGCACTAGGTTTGCCGAGTA-3′);

GAPDH: forward (5′-CCTCGTCCCGTAGACAAAATG-3′) and reverse (5′-TGAGGTCAATGAAGGGGTCGT-3′);

Glyceraldehyde 3-phosphate dehydrogenase (GAPDH) was used as the internal control to normalize the transcript levels of target genes.

Statistical analysis

The data are presented as the means and standard errors of the means and were analyzed statistically using SPSS 17.0 (SPSS Inc., Chicago, IL, USA). The statistical significance was determined using one-way ANOVA followed by Tukey's multiple comparisons test. Two-tailed unpaired t-tests were conducted to compare the two groups. Spearman correlation analysis was conducted to determine the correlation between the bacterial taxa and

the key DEGs. All the statistical tests were conducted using GraphPad Prism 9.0 software (San Diego, CA). The threshold of statistical significance was set to $p < 0.05$.

Data availability

All data needed to evaluate the conclusions in the paper are present in the paper. RNA sequencing data have been deposited in the Sequence Read Archive (SRA) with the accession number PRJNA1112029. The raw reads of 16S rRNA gene amplicon sequencing were deposited into the NCBI Sequence Read Archive database (Accession Number: SRP485545).

Received: 4 June 2024; Accepted: 26 February 2025;
Published online: 25 March 2025

References

1. López-Otín, C., Blasco, M. A., Partridge, L., Serrano, M. & Kroemer, G. The hallmarks of aging. *Cell* **153**, 1194–1217 (2013).
2. Ghosh, T. S., Shanahan, F. & O'Toole, P. W. Toward an improved definition of a healthy microbiome for healthy aging. *Nat. Aging* **2**, 1054–1069 (2022).
3. Salazar, A. M., Aparicio, R., Clark, R. I., Rera, M. & Walker, D.W. Intestinal barrier dysfunction: an evolutionarily conserved hallmark of aging. *Dis. Model Mech.* **16**, dmm049969 (2023).
4. Martins, R. R., McCracken, A. W., Simons, M. J. P., Henriques, C. M. & Rera, M. How to catch a smurf?—Ageing and beyond… In vivo assessment of intestinal permeability in multiple model organisms. *Bio-Protoc.* **8**, e2722 (2018).
5. Meier, J. & Sturm, A. The intestinal epithelial barrier: does it become impaired with age? *Dig. Dis.* **27**, 240–245 (2009).
6. Mitchell, E. L. et al. Reduced intestinal motility, mucosal barrier function, and inflammation in aged monkeys. *J. Nutr. Health Aging* **21**, 354–361 (2017).
7. Man, A. L. et al. Age-associated modifications of intestinal permeability and innate immunity in human small intestine. *Clin. Sci.* **129**, 515–527 (2015).
8. Wu, Y. & Jha, R. Probiotics (*Lactobacillus plantarum* HNU082) supplementation relieves ulcerative colitis by affecting intestinal barrier functions, immunity-related gene expression, gut microbiota, and metabolic pathways in mice. *Microbiol. Spectr.* **10**, e0165122 (2022).
9. Elderman, M. et al. The effect of age on the intestinal mucus thickness, microbiota composition and immunity in relation to sex in mice. *PLoS ONE* **12**, e0184274 (2017).
10. Litvak, Y., Byndloss, M. X. & Bäumler, A. J. Colonocyte metabolism shapes the gut microbiota. *Science* **362**, eaat9076 (2018).
11. Wilmanski, T., Diener, C. & Rappaport, N. Gut microbiome pattern reflects healthy ageing and predicts survival in humans. *Nat. Metab.* **3**, 274–286 (2021).
12. Kong, F., Deng, F., Li, Y. & Zhao, J. Identification of gut microbiome signatures associated with longevity provides a promising modulation target for healthy aging. *Gut Microbes* **10**, 210–215 (2019).
13. Salazar, J. & Durán, P. Exploring the relationship between the gut microbiota and ageing: a possible age modulator. *Int. J. Environ. Res. Public Health* **20**, 5845 (2023).
14. Scott, K. A. et al. Revisiting Metchnikoff: age-related alterations in microbiota-gut-brain axis in the mouse. *Brain Behav. Immun.* **65**, 20–32 (2017).
15. Thevaranjan, N. et al. Age-associated microbial dysbiosis promotes intestinal permeability, systemic inflammation, and macrophage dysfunction. *Cell Host Microbe* **21**, 455–466.e454 (2017).
16. Kigerl, K. A. & Hall, J. C. Gut dysbiosis impairs recovery after spinal cord injury. *J. Exp. Med.* **213**, 2603–2620 (2016).
17. Parker, A. et al. Fecal microbiota transfer between young and aged mice reverses hallmarks of the aging gut, eye, and brain. *Microbiome* **10**, 68 (2022).
18. Boehme, M., Guzzetta, K. E., Bastiaanssen, T. F. S. & van de Wouw, M. Microbiota from young mice counteracts selective age-associated behavioral deficits. *Nat. Aging* **1**, 666–676 (2021).
19. Shin, J. et al. Ageing and rejuvenation models reveal changes in key microbial communities associated with healthy ageing. *Microbiome* **9**, 240 (2021).
20. Han, B. et al. Microbial genetic composition tunes host longevity. *Cell* **169**, 1249–1262.e1213 (2017).
21. Cruz-Pereira, J. S. et al. Age-associated deficits in social behaviour are microbiota-dependent. *Brain Behav. Immun.* **110**, 119–124 (2023).
22. Kyritsis, N. et al. Diagnostic blood RNA profiles for human acute spinal cord injury. *J. Exp. Med.* **218**, e20201795 (2021).
23. Jing, Y. et al. Role of microbiota-gut-brain axis in natural aging-related alterations in behavior. *Front. Neurosci.* **18**, 1362239 (2024).
24. Ren, W. Y. et al. Age-related changes in small intestinal mucosa epithelium architecture and epithelial tight junction in rat models. *Aging Clin. Exp. Res.* **26**, 183–191 (2014).
25. Chelakkot, C., Ghim, J. & Ryu, S. H. Mechanisms regulating intestinal barrier integrity and its pathological implications. *Exp. Mol. Med.* **50**, 1–9 (2018).
26. Tran, L. & Greenwood-Van Meerveld, B. Age-associated remodeling of the intestinal epithelial barrier. *J. Gerontol. A Biol. Sci. Med. Sci.* **68**, 1045–1056 (2013).
27. Zeng, X. et al. Fecal microbiota transplantation from young mice rejuvenates aged hematopoietic stem cells by suppressing inflammation. *Blood* **141**, 1691–1707 (2023).
28. Moore, Y. F., Lambracht-Washington, D., Tabaczewski, P. & Fischer Lindahl, K. Murine MHC class Ib gene, H2-M2, encodes a conserved surface-expressed glycoprotein. *Immunogenetics* **56**, 1–11 (2004).
29. Rahmat-Zaie, R. et al. TNF-α/STAT1/CXCL10 mutual inflammatory axis that contributes to the pathogenesis of experimental models of multiple sclerosis: a promising signaling pathway for targeted therapies. *Cytokine* **168**, 156235 (2023).
30. Finke, D. & Heckmann, M. B. Comparative transcriptomics of immune checkpoint inhibitor myocarditis identifies guanylate binding protein 5 and 6 dysregulation. *Cancers* **13**, 2498 (2021).
31. Xie, D., Hu, J., Wu, T., Cao, K. & Luo, X. Potential biomarkers and drugs for nanoparticle-induced cytotoxicity in the retina: based on regulation of inflammatory and apoptotic genes. *Int. J. Environ. Res. Public Health* **19**, 5664 (2022).
32. Wang, F. T. et al. The role of the CXCR6/CXCL16 axis in the pathogenesis of fibrotic disease. *Int. Immunopharmacol.* **132**, 112015 (2024).
33. Mandai, Y. et al. Distinct roles for $CXCR6^{+}$ and $CXCR6^{-}$ $CD4^{+}$ T cells in the pathogenesis of chronic colitis. *PLoS ONE* **8**, e65488 (2013).
34. Li, H. et al. Glucocorticoid resistance of allogeneic T cells alters the gene expression profile in the inflamed small intestine of mice suffering from acute graft-versus-host disease. *J. Steroid Biochem. Mol. Biol.* **195**, 105485 (2019).
35. Diehl, G. E. et al. Microbiota restricts trafficking of bacteria to mesenteric lymph nodes by CX_3CR1^{hi} cells. *Nature* **494**, 116–120 (2013).
36. Koboziev, I., Karlsson, F. & Grisham, M. B. Gut-associated lymphoid tissue, T cell trafficking, and chronic intestinal inflammation. *Ann. N. Y. Acad. Sci.* **1**, E86–E93 (2010).
37. Shaikh, H. et al. Mesenteric lymph node transplantation in mice to study immune responses of the gastrointestinal tract. *Front. Immunol.* **12**, 689896 (2021).

38. Erofeeva, L. M. & Mnikhovich, M. V. Structural and functional changes in the mesenteric lymph nodes in humans during aging. *Bull. Exp. Biol. Med.* **168**, 694–698 (2020).
39. El Baassiri, M. G. et al. Ccr2-dependent monocytes exacerbate intestinal inflammation and modulate gut serotonergic signaling following traumatic brain injury. *J. Trauma Acute Care Surg.* **97**, 356–364 (2024).
40. Madan, U., Verma, B. & Awasthi, A. Cenicriviroc, a CCR2/CCR5 antagonist, promotes the generation of type 1 regulatory T cells. *Eur. J. Immunol.* **54**, e2350847 (2024).
41. Andres, P. G. et al. Mice with a selective deletion of the CC chemokine receptors 5 or 2 are protected from dextran sodium sulfate-mediated colitis: lack of CC chemokine receptor 5 expression results in a NK1.1+ lymphocyte-associated Th2-type immune response in the intestine. *J. Immunol.* **164**, 6303–6312 (2000).
42. Filippone, R. T., Dargahi, N. & Eri, R. Potent CCR3 receptor antagonist, SB328437, suppresses colonic eosinophil chemotaxis and inflammation in the *Winnie* murine model of spontaneous chronic colitis. *Int. J. Mol. Sci.* **23**, 7780 (2022).
43. Filippone, R. T. et al. Targeting eotaxin-1 and CCR3 receptor alleviates enteric neuropathy and colonic dysfunction in TNBS-induced colitis in guinea pigs. *Neurogastroenterol. Motil.* **30**, e13391 (2018).
44. Moratalla, A. et al. *Bifidobacterium pseudocatenulatum* CECT7765 promotes a TLR2-dependent anti-inflammatory response in intestinal lymphocytes from mice with cirrhosis. *Eur. J. Nutr.* **55**, 197–206 (2016).
45. Walrath, T. et al. IFN-γ and IL-17A regulate intestinal crypt production of CXCL10 in the healthy and inflamed colon. *Am. J. Physiol. Gastrointest. Liver Physiol.* **318**, G479–G489 (2020).
46. Yu, M. et al. Aryl hydrocarbon receptor activation modulates intestinal epithelial barrier function by maintaining tight junction integrity. *Int. J. Biol. Sci.* **14**, 69–77 (2018).
47. James, K. R. & Gomes, T. Distinct microbial and immune niches of the human colon. *Nat. Immunol.* **21**, 343–353 (2020).
48. Halfvarson, J. et al. Dynamics of the human gut microbiome in inflammatory bowel disease. *Nat. Microbiol.* **2**, 17004 (2017).
49. Conway, J. & N, A. D. Ageing of the gut microbiome: potential influences on immune senescence and inflammageing. *Ageing Res. Rev.* **68**, 101323 (2021).
50. Kang, L. et al. L-arabinose attenuates LPS-induced intestinal inflammation and injury through reduced M1 macrophage polarization. *J. Nutr.* **153**, 3327–3340 (2023).
51. Wu, Y. et al. Deferasirox alleviates DSS-induced ulcerative colitis in mice by inhibiting ferroptosis and improving intestinal microbiota. *Life Sci.* **314**, 121312 (2023).
52. Zhang, Y. et al. *Dubosiella newyorkensis* modulates immune tolerance in colitis via the L-lysine-activated AhR-IDO1-Kyn pathway. *Nat. Commun.* **15**, 1333 (2024).
53. Parker, B. J., Wearsch, P. A., Veloo, A. C. M. & Rodriguez-Palacios, A. The genus *Alistipes*: gut bacteria with emerging implications to inflammation, cancer, and mental health. *Front. Immunol.* **11**, 906 (2020).
54. Wexler, H. M. Bacteroides: the good, the bad, and the nitty-gritty. *Clin. Microbiol Rev.* **20**, 593–621 (2007).
55. Zafar, H. & Saier, M. H. Jr Gut *Bacteroides* species in health and disease. *Gut Microbes* **13**, 1–20 (2021).
56. Gu, K. et al. Iron overload induces colitis by modulating ferroptosis and interfering gut microbiota in mice. *Sci. Total Environ.* **905**, 167043 (2023).
57. Ding, N. et al. Impairment of spermatogenesis and sperm motility by the high-fat diet-induced dysbiosis of gut microbes. *Gut* **69**, 1608–1619 (2020).
58. Wan, Y. et al. Effects of dietary fat on gut microbiota and faecal metabolites, and their relationship with cardiometabolic risk factors: a 6-month randomised controlled-feeding trial. *Gut* **68**, 1417–1429 (2019).
59. Liu, Q. & Johnson, E. M. Peripheral TREM1 responses to brain and intestinal immunogens amplify stroke severity. *Nat. Immunol.* **20**, 1023–1034 (2019).
60. Yu, X. et al. Gut microbiota dysbiosis induced by intracerebral hemorrhage aggravates neuroinflammation in mice. *Front. Microbiol.* **12**, 647304 (2021).
61. Singh, V. & Roth, S. Microbiota dysbiosis controls the neuroinflammatory response after stroke. *J. Neurosci.* **36**, 7428–7440 (2016).
62. Fransen, F. et al. Aged gut microbiota contributes to systemical inflammaging after transfer to germ-free mice. *Front. Immunol.* **8**, 1385 (2017).
63. Rath, E. & Haller, D. Intestinal epithelial cell metabolism at the interface of microbial dysbiosis and tissue injury. *Mucosal Immunol.* **15**, 595–604 (2022).
64. Takeuchi, T. et al. Fatty acid overproduction by gut commensal microbiota exacerbates obesity. *Cell Metab.* **35**, 361–375.e369 (2023).
65. Miyamoto, K. et al. The gut microbiota-induced kynurenic acid recruits GPR35-positive macrophages to promote experimental encephalitis. *Cell Rep.* **42**, 113005 (2023).
66. Otake-Kasamoto, Y. & Kayama, H. Lysophosphatidylserines derived from microbiota in Crohn's disease elicit pathological Th1 response. *J. Exp. Med.* **219**, e20211291 (2022).
67. Chen, S., Zhou, Y., Chen, Y. & Gu, J. fastp: an ultra-fast all-in-one FASTQ preprocessor. *Bioinformatics* **34**, i884–i890 (2018).
68. Kim, D., Langmead, B. & Salzberg, S. L. HISAT: a fast spliced aligner with low memory requirements. *Nat. Methods* **12**, 357–360 (2015).
69. Pertea, M. et al. StringTie enables improved reconstruction of a transcriptome from RNA-seq reads. *Nat. Biotechnol.* **33**, 290–295 (2015).
70. Love, M. I., Huber, W. & Anders, S. Moderated estimation of fold change and dispersion for RNA-seq data with DESeq2. *Genome Biol.* **15**, 550 (2014).
71. Xie, C. et al. KOBAS 2.0: a web server for annotation and identification of enriched pathways and diseases. *Nucleic Acids Res.* **39**, W316–W322 (2011).
72. Boscaini, S. et al. Depletion of the gut microbiota differentially affects the impact of whey protein on high-fat diet-induced obesity and intestinal permeability. *Physiol. Rep.* **9**, e14867 (2021).
73. Jing, Y. et al. Effect of fecal microbiota transplantation on neurological restoration in a spinal cord injury mouse model: involvement of brain-gut axis. *Microbiome* **9**, 59 (2021).

Acknowledgements

The present study was funded by the National Natural Science Foundation of China [grant numbers 82271433, 81901272]; the Special Fund for Basic Scientific Research of Central Public Research Institutes [grant numbers 2022cz-5]. The funder played no role in the study design, data collection, analysis and interpretation of data, or the writing of this manuscript.

Author contributions

Y.Y. and Y.J. were responsible for the study conception and direction. Y.J. and Q.W. were in charge of experimental design, result interpretation, and manuscript writing. Y.J., F.B. and Q.W. were responsible for animal experiments as well as data acquisition. Y.L., S.Z. and C.G. carried out behavioral tests and histological analysis together with biochemical experiments. W.L. and Y.Y. contributed to the data analysis. Z.L. and F.B. were in charge of manuscript revision. All authors read and approved the final manuscript.

Competing interests
The authors declare no competing interests.

Additional information
Supplementary information The online version contains supplementary material available at https://doi.org/10.1038/s41522-025-00677-y.

Correspondence and requests for materials should be addressed to Yan Yu.